This is a preprint of an article accepted for publication in the Journal of Advances in Engineering Software on 21 June 2011. The published article is available online at http://www.sciencedirect.com/science/article/pii/S0965997811001827
To be cited as: Bouaanani N., Ighouba M. 2011. A novel scheme for large deflection analysis of suspended cables made of linear or nonlinear elastic materials. Journal of Advances in Engineering Software, Vol. 42, No. 12, 1009-1019.

# A novel scheme for large deflection analysis of suspended cables made of linear or nonlinear elastic materials

Najib Bouaanani [1] and Mohamed Ighouba [2]

**Abstract:** This paper presents a new approach to investigate the static response of horizontal and inclined suspended cables with deformable cross-section, made of general linear or nonlinear elastic materials, and subjected to vertical concentrated and distributed loads. The proposed technique also includes large sag and extensibility effects, and is based on an original finite difference scheme combined to a nonlinear least squares numerical solution. The mathematical formulation is developed for various loading cases, and an innovative computational strategy is used to transform the resulting nonlinear system of equations into a scaled nonlinear least squares problem. The numerical scheme is programmed and its application illustrated through examples highlighting the effects of coupling between the tension in a cable and the deformation of its cross-section as well as the use of cables made of neo-Hookean materials. The results obtained are in excellent agreement with analytical solutions when available. The proposed technique can be easily programmed and constitutes a valuable tool for large deflection analysis of suspended cables made of nonlinear elastic materials.

**Key words:** Suspended cables; Nonlinear elasticity; Finite differences method; Large deflections; Numerical methods; nonlinear least squares problems; Neo-Hookean materials; Rubber-like materials.

[1] Professor, Department of Civil, Geological and Mining Engineering,
École Polytechnique de Montréal, Montréal, QC H3C 3A7, Canada
Corresponding author. E-mail: najib.bouaanani@polymtl.ca
[2] Research Assistant, Department of Civil, Geological and Mining Engineering,
École Polytechnique de Montréal, Montréal, QC H3C 3A7, Canada.

# 1 Introduction

Cables are widely used as structural components and the investigation of their structural response has attracted numerous researchers for many centuries [1–3]. Most of these contributions accounted only for simplified loading cases and focused on validating the parabolic or catenary cable solutions amenable to hand calculations. With the advent of digital computers, advanced analytical and numerical techniques emerged as practical solutions to study cables under various loading cases, such as in [3–13] and more recently in [14–22]. Existing finite element software packages that solve cable problems generally use truss or beam elements including large displacement capabilities, i.e. geometrical nonlinearity. Such elements are highly effective solutions that avoid recourse to cumbersome cable modeling using 3D solid finite elements. However, the truss and beam formulations programmed into readily available finite element softwares are generally restricted to linear elastic Hookean materials, and do not allow for straightforward implementation of general constitutive nonlinear material models to account for hyper-elastic or rubber-like materials. Furthermore, these classical formulations do not account for coupling between the tension in a cable and the deformation of its cross-section which is assumed to remain rigid as the loads are applied. In this paper, we propose alternative finite difference solutions that waive these restricting assumptions. Finite difference modeling of cables was indeed shown very effective in many cable applications such as transmission lines, marine cables and cable-supported bridges [23–32]. Such studies showed that finite difference schemes can be easily programmed to yield robust numerical solutions and that their use is particularly justified when discretized nondimensional equations are to be solved systematically for problem parameters varying over a wide range. However, the available finite difference formulations for cables also employ a simplifying rigid cross-section kinematic assumption and are limited to linear Hookean materials.

The objective of this work is to develop an original and practical finite difference scheme to investigate the static response of horizontal and inclined suspended cables with deformable cross-section, made of general linear or nonlinear elastic materials, and subjected to most common loads of gravitational type, generally originating from self-weight, ice accumulation or various attachements. The proposed formulation also includes large sag and extensibility effects that were shown sufficiently important to include in the analysis of cables when large spans and/or significant loads are involved such as for applications described in [33–38].

# 2 Mathematical and numerical formulations

## 2.1 Cable static response under self-weight

### *2.1.1 Mathematical formulation*

In this section, we derive the Cartesian equations expressing the static profile of a suspended cable hanging under its self-weight as illustrated in Fig. 1. Considering a Cartesian system of axes $(x, y, z)$,

the cable is assumed to deflect within the plane $(x, z)$. We note $(x_{\mathrm{A}}, y_{\mathrm{A}}, z_{\mathrm{A}})$ and $(x_{\mathrm{B}}, y_{\mathrm{B}}, z_{\mathrm{B}})$ the coordinates of the two cable supports A and B, respectively. To alleviate the notation, we may assume without loss of generality that support A coincides with the origin of axes, i.e. $x_{\mathrm{A}} = y_{\mathrm{A}} = z_{\mathrm{A}} = 0$. The chord connecting the supports A and B makes an angle $\theta$ with the $x$-axis. We note $\widetilde{S}$ the unstrained arc-length of the cable, and $\widetilde{m}\mathrm{g}$ its weight per unit unstrained arc-length with g representing the gravity constant. The Lagrangian coordinate of a point of the cable in its unstrained configuration is denoted by $\widetilde{s}$. The static strained geometrical configuration is obtained when the cable deforms under self-weight. We note $\widehat{S}$ the strained arc-length of the cable, $\widehat{m}\mathrm{g}$ the weight of the cable per unit strained arc-length and $\widehat{s}$ the Lagrangian coordinate of a point of the cable in the strained configuration.

Fig. 1 (a) illustrates the strained geometrical configuration of the suspended cable and the forces applied to an elementary segment of the cable with infinitesimal arc-length $\mathrm{d}\widehat{s}$. Let $\widehat{F}$ denote the tension force at a point with Lagrangian coordinate $\widehat{s}$ and Cartesian coordinate $\widehat{x}$. At coordinates $\widehat{s} + \mathrm{d}\widehat{s}$ and $x + \mathrm{d}x$, the tension force is $\widehat{F} + \mathrm{d}\widehat{F}$. The horizontal and vertical projections of the cable tensions $\widehat{F}$ and $\widehat{F} + \mathrm{d}\widehat{F}$ are designated by $\widehat{H}$, $\widehat{V}$, $\widehat{H} + \mathrm{d}\widehat{H}$ and $\widehat{V} + \mathrm{d}\widehat{V}$ as illustrated in Fig. 1 (a). The equilibrium of the elementary segment yields

$$\mathrm{d}\widehat{H} = 0 \tag{1}$$

$$\frac{\mathrm{d}\widehat{V}}{\mathrm{d}\widehat{x}} = -\widehat{m}\mathrm{g}\sqrt{1 + \left(\frac{\mathrm{d}\widehat{z}}{\mathrm{d}\widehat{x}}\right)^2} \tag{2}$$

$$\widehat{H}\,\frac{\mathrm{d}\widehat{z}}{\mathrm{d}\widehat{x}} - \widehat{V} = 0 \tag{3}$$

Eq. (1) shows that horizontal tension $\widehat{H}$ is constant along cable arc-length, and the last two relations yield

$$\widehat{H}\widehat{z}'' + \widehat{m}\mathrm{g}\sqrt{1 + (\widehat{z}')^2} = 0 \tag{4}$$

where the notations $\widehat{z}' = \mathrm{d}\widehat{z}/\mathrm{d}\widehat{x}$ and $\widehat{z}'' = \mathrm{d}^2\widehat{z}/\mathrm{d}\widehat{x}^2$ are used to alleviate the text. The tension force $\widehat{F}$ can be decomposed as

$$\widehat{F} = \widehat{H}\cos\widehat{\phi} + \widehat{V}\sin\widehat{\phi} = \widehat{H}\,\frac{\mathrm{d}\widehat{x}}{\mathrm{d}\widehat{s}} + \widehat{V}\,\frac{\mathrm{d}\widehat{z}}{\mathrm{d}\widehat{s}} \tag{5}$$

in which $\widehat{\phi}$ is the angle between the tangent to the cable profile and a horizontal axis as illustrated in Fig. 1 (a). Using Eqs. (1) to (3) and (5), we obtain

$$\widehat{F} = \widehat{H}\,\frac{\mathrm{d}\widehat{x}}{\mathrm{d}\widehat{s}} + \left(\widehat{H}\,\frac{\mathrm{d}\widehat{z}}{\mathrm{d}\widehat{x}}\right)\frac{\mathrm{d}\widehat{z}}{\mathrm{d}\widehat{s}} = \widehat{H}\sqrt{1 + (\widehat{z}')^2} \tag{6}$$

The masses $\widetilde{m}$ and $\widehat{m}$ are distributed per unit unstrained and strained arc-lengths, respectively, and are related by

$$\widehat{m} = \widetilde{m}\,\frac{\mathrm{d}\widetilde{s}}{\mathrm{d}\widehat{s}} \tag{7}$$

and axial deformation can be characterized along cable arc-length by

$$\frac{\mathrm{d}\widehat{s} - \mathrm{d}\widetilde{s}}{\mathrm{d}\widetilde{s}} = \mathcal{C}(\widehat{\tau}) \tag{8}$$

in which

$$\widehat{\tau} = \frac{\widehat{F}}{EA} = \frac{\widehat{H}}{EA}\sqrt{1 + (\widehat{z}\,')^2} \tag{9}$$

and where $A$ is the area of the cable cross-section, $E$ is the modulus of elasticity and $\mathcal{C}$ is a general constitutive function characterizing cable axial deformation. For example, $\mathcal{C}$ can be expressed in the simple case of a Hookean material as

$$\mathcal{C}(\widehat{\tau}) = \widehat{\tau} \tag{10}$$

More complex expressions of $\mathcal{C}$ will be investigated later in Section 3 of this paper.

Using Eq. (8), Eq. (7) becomes

$$\widehat{m} = \frac{\widetilde{m}}{1 + \mathcal{C}(\widehat{\tau})} \tag{11}$$

Substituting Eqs. (11) and (6) into Eq. (4) yields the nonlinear differential equation governing the static profile of the cable including extensibility and large sag effects

$$\widehat{H}\,\widehat{z}\,'' + \frac{\widetilde{m}\mathrm{g}\sqrt{1 + (\widehat{z}\,')^2}}{1 + \mathcal{C}\left(\widehat{\mu}\sqrt{1 + (\widehat{z}\,')^2}\right)} = 0 \tag{12}$$

where $\widehat{\mu}$ is a nondimensional parameter given by

$$\widehat{\mu} = \frac{\widehat{H}}{EA} \tag{13}$$

Eq. (12) accounts for large sag, extensibility and material behavior effects while expressing the nonlinear static profile of a suspended cable in Cartesian coordinates instead of Lagrangian coordinates used in most formulations reported in the literature. This formulation will be used to develop the finite difference scheme presented next.

### *2.1.2 Finite difference discretization*

A finite difference scheme will be used to solve Eq. (12) numerically for the static deflections $\widehat{z}$ and horizontal component of cable tension $\widehat{H}$. Prior to discretization, an appropriate scaling must be applied to ensure a well-conditioned system and numerical convergence as will be discussed later. For that purpose, we introduce the nondimensional parameters

$$\widehat{X} = \frac{\widehat{x}}{L}; \qquad \widehat{Z} = \frac{\widehat{z}}{L}; \qquad \widehat{f}_0 = \frac{\widetilde{m}\mathrm{g}L}{8\widehat{H}} \tag{14}$$

and rewrite Eq. (12) as

$$\widehat{Z}'' + \frac{8\widehat{f}_0\sqrt{1+\left(\widehat{Z}'\right)^2}}{1+\mathcal{C}\left(\frac{\zeta}{\widehat{f}_0}\sqrt{1+\left(\widehat{Z}'\right)^2}\right)} = 0 \tag{15}$$

where

$$\zeta = \frac{\widetilde{m}\mathrm{g}L}{8EA} \tag{16}$$

The suspended cable is then discretized into $N_\mathrm{e}$ equal length finite difference elements corresponding to $n = N_\mathrm{e} - 1$ interior nodes as illustrated in Fig. 1 (b). Using a central finite difference scheme, Eq. (15) is transformed into a system of $n$ nonlinear equations expressed at each interior node $i$, $i = 1 \ldots n$, as

$$\eta_i = b_i + \frac{8\widehat{f}_0\sqrt{h_i}}{1+\mathcal{C}_i\left(\widehat{f}_0\right)} = 0 \tag{17}$$

where the coefficients $a_i$, $b_i$, $h_i$ and $\mathcal{C}_i$ are defined at node $i$ of the finite difference mesh as

$$a_i = \frac{1}{2}\left(n+1\right)\left(\widehat{Z}_{i+1} - \widehat{Z}_{i-1}\right) \tag{18}$$

$$b_i = \left(n+1\right)^2\left(\widehat{Z}_{i+1} - 2\,\widehat{Z}_i + \widehat{Z}_{i-1}\right) \tag{19}$$

$$h_i = 1 + a_i^2 \tag{20}$$

$$\mathcal{C}_i\left(\widehat{f}_0\right) = \mathcal{C}\left(\frac{\zeta}{\widehat{f}_0}\sqrt{h_i}\right) \tag{21}$$

in which $\widehat{Z}_i$ denotes the nondimensional static deflection at node $i$. The values of these parameters at nodes $i = 1$ and $i = n$ of the finite difference mesh are obtained by imposing the boundary conditions at both ends of the cable, yielding

$$a_1 = \frac{1}{2}\left(n+1\right)\widehat{Z}_2 \tag{22}$$

$$a_n = \frac{1}{2}\left(n+1\right)\left(\tan\theta - \widehat{Z}_{n-1}\right) \tag{23}$$

$$b_1 = \left(n+1\right)^2\left(\widehat{Z}_2 - 2\,\widehat{Z}_1\right) \tag{24}$$

$$b_n = \left(n+1\right)^2\left(\tan\theta - 2\,\widehat{Z}_n + \widehat{Z}_{n-1}\right) \tag{25}$$

Eqs. (17) are not sufficient to determine cable response unless horizontal tension $\widehat{H}$ is known, which is not the case in general. Eqs. (17) have then to be complemented by an additional relation involving $\widehat{H}$ to uniquely define the cable's static profile. This relation is obtained here by equating the computed unstrained arc-length of the cable to the given initial unstrained arc-length $\widetilde{S}$, yielding the nondimen-

sional constraint equation

$$\eta_{n+1} = \frac{1}{n+1} \sum_{j=1}^{n+1} \frac{\sqrt{1+\kappa_j^2}}{1+\varepsilon_j} - \frac{\widetilde{S}}{L} = 0 \tag{26}$$

where for $j = 1 \dots n+1$

$$\kappa_j = \big(n+1\big)\big(\widehat{Z}_j - \widehat{Z}_{j-1}\big) \tag{27}$$

and

$$\varepsilon_j = \frac{1}{2}\Big[\mathcal{C}_{j-1}\big(\widehat{f}_0\big) + \mathcal{C}_j\big(\widehat{f}_0\big)\Big] \tag{28}$$

with

$$\mathcal{C}_0\big(\widehat{f}_0\big) = \mathcal{C}\left(\frac{\zeta}{\widehat{f}_0}\sqrt{h_0}\right) \tag{29}$$

$$\mathcal{C}_{n+1}\big(\widehat{f}_0\big) = \mathcal{C}\left(\frac{\zeta}{\widehat{f}_0}\sqrt{h_{n+1}}\right) \tag{30}$$

in which coefficients $h_0$ to $h_{n+1}$ are obtained from Eq. (20) considering

$$a_0 = \big(n+1\big)\,\widehat{Z}_1 \tag{31}$$

$$a_{n+1} = \big(n+1\big)\big(\tan\theta - \widehat{Z}_n\big) \tag{32}$$

$$b_0 = 0 \tag{33}$$

$$b_{n+1} = 0 \tag{34}$$

We note that the strained arc-length of the cable can be expressed as

$$\widehat{S} = \frac{L}{n+1} \sum_{j=1}^{n+1} \sqrt{1+\kappa_j^2} \tag{35}$$

Eqs. (17) and (26) can be solved numerically to find deflections $\widehat{Z}_i$, $i = 1 \dots n$, and the nondimensional parameter $\widehat{f}_0$. Eq. (14) can then be used to obtain the horizontal tension $\widehat{H}$. Although the above equations could be solved directly for $\widehat{H}$ without scaling through $\widehat{f}_0$ in theory, this process generally affects the well-conditioning and therefore the convergence of the numerical scheme because of large differences in the magnitudes of the variables $\widehat{Z}_i$, $i = 1 \dots n$, $\widehat{H}$ and their derivatives. The scaling introduced is efficient since cable deflections and sag are generally of the same order of magnitude.

Classical Newton-Raphson or shooting method algorithms can be used to solve Eqs. (17) and (26) numerically. In this work, another innovative computational strategy is used where the equations are first transformed into a nonlinear least squares (NLS) problem consisting of finding the vector $\boldsymbol{\chi}$ of unknowns $\widehat{Z}_i$, $i = 1 \dots n$, and $\widehat{f}_0$

$$\boldsymbol{\chi} = \Big[\widehat{Z}_1, \widehat{Z}_2, \dots, \widehat{Z}_i, \dots, \widehat{Z}_n, \widehat{f}_0\Big]^{\mathrm{T}} \tag{36}$$

that minimizes the sum

$$\sum_{i=1}^{n+1} \eta_i^2 = \Big( \|\boldsymbol{\eta}\|_2 \Big)^2 \tag{37}$$

where $\|.\|_2$ denotes the Euclidian vector norm and where the vector $\boldsymbol{\eta}$ is given by

$$\boldsymbol{\eta} = \Big[ \eta_1, \eta_2, \ldots, \eta_i, \ldots, \eta_n, \eta_{n+1} \Big]^{\mathrm{T}} \tag{38}$$

in which functions $\eta_1$ to $\eta_n$ are defined by Eqs. (17), while function $\eta_{n+1}$ is given by Eq. (26). The resulting NLS problem is solved herein by applying a Gauss–Newton algorithm. Staring with an initial guess vector $\boldsymbol{\chi}^{(0)}$, incremental solutions are obtained at iteration $\ell + 1$ as

$$\boldsymbol{\chi}^{(\ell+1)} = \boldsymbol{\chi}^{(\ell)} - \Big[ \mathbf{J}_{\boldsymbol{\eta}^{(\ell)}}^{\mathrm{T}} \, \mathbf{J}_{\boldsymbol{\eta}^{(\ell)}} \Big]^{-1} \mathbf{J}_{\boldsymbol{\eta}^{(\ell)}}^{\mathrm{T}} \, \boldsymbol{\eta}^{(\ell)} \tag{39}$$

in which vectors $\boldsymbol{\chi}^{(\ell)}$ and $\boldsymbol{\eta}^{(\ell)}$ correspond to iteration $\ell$, and where $\mathbf{J}_{\boldsymbol{\eta}^{(\ell)}}$ denotes the $(n+1) \times (n+1)$ Jacobian matrix of $\boldsymbol{\eta}^{(\ell)}$ with respect to $\boldsymbol{\chi}^{(\ell)}$, given by

$$\mathbf{J}_{\boldsymbol{\eta}^{(\ell)}} = \begin{bmatrix} \dfrac{\partial \eta_1^{(\ell)}}{\partial \widehat{Z}_1^{(\ell)}} & \cdots & \dfrac{\partial \eta_1^{(\ell)}}{\partial \widehat{Z}_i^{(\ell)}} & \cdots & \dfrac{\partial \eta_1^{(\ell)}}{\partial \widehat{Z}_n^{(\ell)}} & \dfrac{\partial \eta_1^{(\ell)}}{\partial \widehat{f}_0^{(\ell)}} \\ \dfrac{\partial \eta_2^{(\ell)}}{\partial \widehat{Z}_1^{(\ell)}} & \cdots & \dfrac{\partial \eta_2^{(\ell)}}{\partial \widehat{Z}_i^{(\ell)}} & \cdots & \dfrac{\partial \eta_2^{(\ell)}}{\partial \widehat{Z}_n^{(\ell)}} & \dfrac{\partial \eta_2^{(\ell)}}{\partial \widehat{f}_0^{(\ell)}} \\ \vdots & \ddots & \vdots & \ddots & \vdots & \vdots \\ \dfrac{\partial \eta_i^{(\ell)}}{\partial \widehat{Z}_1^{(\ell)}} & \cdots & \dfrac{\partial \eta_i^{(\ell)}}{\partial \widehat{Z}_i^{(\ell)}} & \cdots & \dfrac{\partial \eta_i^{(\ell)}}{\partial \widehat{Z}_n^{(\ell)}} & \dfrac{\partial \eta_i^{(\ell)}}{\partial \widehat{f}_0^{(\ell)}} \\ \vdots & \ddots & \vdots & \ddots & \vdots & \vdots \\ \dfrac{\partial \eta_n^{(\ell)}}{\partial \widehat{Z}_1^{(\ell)}} & \cdots & \dfrac{\partial \eta_n^{(\ell)}}{\partial \widehat{Z}_i^{(\ell)}} & \cdots & \dfrac{\partial \eta_n^{(\ell)}}{\partial \widehat{Z}_n^{(\ell)}} & \dfrac{\partial \eta_n^{(\ell)}}{\partial \widehat{f}_0^{(\ell)}} \\ \dfrac{\partial \eta_{n+1}^{(\ell)}}{\partial \widehat{Z}_1^{(\ell)}} & \cdots & \dfrac{\partial \eta_{n+1}^{(\ell)}}{\partial \widehat{Z}_i^{(\ell)}} & \cdots & \dfrac{\partial \eta_{n+1}^{(\ell)}}{\partial \widehat{Z}_n^{(\ell)}} & \dfrac{\partial \eta_{n+1}^{(\ell)}}{\partial \widehat{f}_0^{(\ell)}} \end{bmatrix} \tag{40}$$

The proposed procedure consisting of transforming cable equations to a NLS problem and solving it numerically by applying a Gauss–Newton algorithm is more effective than the Newton-Raphson technique since only first-order derivatives are needed to construct the Jacobian matrix $\mathbf{J}_{\boldsymbol{\eta}^{(\ell)}}$. We also show that the Gauss–Newton algorithm satisfies local quadratic convergence when applied to a zero-residual problem as in the present case [40]. Furthermore, the non-null terms of the Jacobian matrix can be obtained easily using the analytical expressions proposed in Appendix A.

## 2.2 Effect of additional distributed and concentrated loads

Fig. 2 illustrates a suspended cable subjected to: (i) self-weight, and (ii) vertical loads $Q^{(k)}$, $k = 1 \ldots N_Q$, uniformly distributed per unit arc-length between nodes $q_1^{(k)}$ and $q_2^{(k)}$ with $1 \leqslant q_1^{(k)} < q_2^{(k)} \leqslant n$, and (iii) vertical concentrated loads $P^{(k)}$, $k = 1 \ldots N_P$, applied at nodes $p^{(k)}$ with $1 \leqslant p^{(k)} \leqslant n$. At each interior node $i$, we define a nondimensional parameter $\widehat{f}_i$

$$\widehat{f}_i = \begin{cases} \dfrac{L}{8\widehat{H}} \left[ \widetilde{m}\mathrm{g} + \dfrac{Q^{(k)}}{2} \right] \text{ if } i = q_1^{(k)} \text{ or } i = q_2^{(k)} & (41) \\ \dfrac{L}{8\widehat{H}} \left[ \widetilde{m}\mathrm{g} + Q^{(k)} \right] \text{ if } q_1^{(k)} < i < q_2^{(k)} & (42) \\ \dfrac{\widetilde{m}\mathrm{g}L}{8\widehat{H}} \qquad \text{otherwise} & (43) \end{cases}$$

We also introduce the nondimensional parameter $\widehat{f}_Q$

$$\widehat{f}_Q = \frac{L}{8\widehat{H}} \left( \widetilde{m}\mathrm{g} + Q \right) \tag{44}$$

where $Q = \sum_{k=1}^{N_Q} Q^{(k)}$.

We show that the nonlinear equations resulting from finite difference discretization can now be expressed at each interior node $i$, $i = 1 \ldots n$, as

$$\eta_i = \begin{cases} b_i + \dfrac{8\widehat{f}_i \sqrt{h_i}}{1 + \mathcal{C}_i\left(\widehat{f}_Q\right)} \\ \quad + \dfrac{8\,(n+1)\,\widehat{f}_Q\,P^{(k)}}{L\left(\widetilde{m}\mathrm{g} + Q\right)} = 0 \quad \text{if } i = p^{(k)} & (45) \\ b_i + \dfrac{8\widehat{f}_i \sqrt{h_i}}{1 + \mathcal{C}_i\left(\widehat{f}_Q\right)} = 0 \qquad \text{otherwise} & (46) \end{cases}$$

in which

$$\mathcal{C}_i\left(\widehat{f}_Q\right) = \mathcal{C}\left( \frac{\zeta}{\widehat{f}_Q} \sqrt{h_i} \right) \tag{47}$$

Eqs. (45) and (46) must be complemented by Eq. (26) in which

$$\varepsilon_j = \frac{1}{2} \left[ \mathcal{C}_{j-1}\left(\widehat{f}_Q\right) + \mathcal{C}_j\left(\widehat{f}_Q\right) \right] \tag{48}$$

with

$$\mathcal{C}_0\left(\widehat{f}_Q\right) = \mathcal{C}\left(\frac{\zeta}{\widehat{f}_Q}\sqrt{h_0}\right) \tag{49}$$

$$\mathcal{C}_{n+1}\left(\widehat{f}_Q\right) = \mathcal{C}\left(\frac{\zeta}{\widehat{f}_Q}\sqrt{h_{n+1}}\right) \tag{50}$$

in which coefficients $h_0$ to $h_{n+1}$ are obtained from Eqs. (20), (22)-(23) and (31)-(32).

Eqs. (45), (46) and (26) can be transformed into a NLS problem as described before through Eqs. (36) to (38), and a Gauss–Newton algorithm can be applied [Eqs. (39) and (40)]. To avoid bad-conditioning, the NLS problem has to be solved for the vector $\boldsymbol{\chi}$

$$\boldsymbol{\chi} = \left[\widehat{Z}_1, \widehat{Z}_2, \ldots, \widehat{Z}_i, \ldots, \widehat{Z}_n, \widehat{f}_Q\right]^{\mathrm{T}} \tag{51}$$

which is the same as the solution vector in Eq. (36) but with the parameter $\widehat{f}_0$ replaced by the parameter $\widehat{f}_Q$ obtained from Eq. (44). Also, the Jacobian matrix $\mathbf{J}_{\boldsymbol{\eta}^{(\ell)}}$ is obtained from Eq. (40) but replacing $\widehat{f}_0$ by the parameter $\widehat{f}_Q$. The analytical expressions of the non-null terms of the Jacobian matrix $\mathbf{J}_{\boldsymbol{\eta}^{(\ell)}}$ are given in Appendix B.

## 3 Numerical implementation and validation examples

### 3.1 Numerical implementation

The developed mathematical formulations and finite difference schemes described above were programmed using MATLAB ® [39]. The flowchart in Fig. 3 illustrates the proposed methodology and the different steps to investigate the static response of suspended cables subjected to self-weight, and vertical concentrated and uniformly distributed loads. For clarity, the flowchart refers to equation numbers from the previous sections. When the cable is subjected only to self-weight, the flowchart in Fig. 3 can be applied using $P^{(k)} = 0$, $Q = 0$ and replacing $\widehat{f}_Q$ by $\widehat{f}_0$.

The starting guess solution of an iterative numerical scheme is generally based on a reasonable estimate of the solution by the analyst. Non-dimensionalizing the problem as described previously not only adresses bad-scaling effects due to widely differing magnitudes of the variables and their derivatives, but it also confines the solutions and therefore the starting initial guess around relatively small values corresponding to commonly encountered deflections normalized by cable span [3,13]. The convergence of the numerical model can be verified by selecting a very small upper-bound value $TOL$ of the infinity norm $\|\boldsymbol{\eta}\|_\infty = \max_i |\eta_i|$, and ending the iterations when $\|\boldsymbol{\eta}\|_\infty \leqslant TOL$. Other convergence criteria based on the minimization of the error on cable deflections and horizontal tension can also be implemented easily in the computational scheme.

To illustrate the application of the methodology and the important aspects of the proposed computational model, the following examples investigate the nonlinear static response of horizontal and inclined suspended cables subjected to self-weight and to vertical concentrated and uniformly distributed loads. The results obtained are validated against analytical solutions when available.

### 3.2 Application to the analysis of Hookean cables including cross-sectional deformations

The analysis of suspended cables is generally conducted assuming that their cross-section remains rigid and therefore neglecting the effect of cross-sectional deformations on the cable's deflected profile and tension. Some authors waived this assumption by including the contraction of cable's cross-section due to Poisson's effect [14, 17, 41]. In this case, we show that Hooke's law can be expressed in terms of Poisson's ratio $\nu$ and the function $\mathcal{C}$ in Eq. (8) as

$$\widehat{F} = EA\left[1 - \nu\,\mathcal{C}(\widehat{\tau})\right]^2 \mathcal{C}(\widehat{\tau}) \tag{52}$$

or using Eq. (9)

$$\mathcal{C}(\widehat{\tau}) - 2\nu\left[\mathcal{C}(\widehat{\tau})\right]^2 + \nu^2\left[\mathcal{C}(\widehat{\tau})\right]^3 = \widehat{\tau} \tag{53}$$

which can be solved for $\mathcal{C}(\widehat{\tau})$ numerically or analytically using Cardano's formula. Differentiating Eq. (53) with respect to $\widehat{Z}$, $\widehat{f}_0$ and $\widehat{f}_Q$ gives

$$\frac{\partial \mathcal{C}(\widehat{\tau})}{\partial \widehat{Z}} = \Gamma(\widehat{\tau})\,\frac{\partial \widehat{\tau}}{\partial \widehat{Z}} \tag{54}$$

$$\frac{\partial \mathcal{C}(\widehat{\tau})}{\partial \widehat{f}_0} = \Gamma(\widehat{\tau})\,\frac{\partial \widehat{\tau}}{\partial \widehat{f}_0} \tag{55}$$

$$\frac{\partial \mathcal{C}(\widehat{\tau})}{\partial \widehat{f}_Q} = \Gamma(\widehat{\tau})\,\frac{\partial \widehat{\tau}}{\partial \widehat{f}_Q} \tag{56}$$

in which

$$\Gamma(\widehat{\tau}) = \frac{1}{1 - 4\nu\,\mathcal{C}(\widehat{\tau}) + 3\nu^2\left[\mathcal{C}(\widehat{\tau})\right]^2} \tag{57}$$

Then, using Eqs. (9), (14) and (44), we obtain the derivatives

$$\frac{\partial \mathcal{C}_i\left(\widehat{f}_0\right)}{\partial \widehat{Z}_j} = \frac{\zeta\,\Gamma_i(\widehat{f}_0)}{\widehat{f}_0}\,\frac{\partial \sqrt{h_i}}{\partial \widehat{Z}_j} \quad \text{for } i, j = 1 \ldots n \tag{58}$$

$$\frac{\partial \mathcal{C}_i\left(\widehat{f}_0\right)}{\partial \widehat{f}_0} = -\frac{\zeta\,\Gamma_i(\widehat{f}_0)}{\widehat{f}_0^2}\,\sqrt{h_i} \quad \text{for } i = 0 \ldots n+1 \tag{59}$$

required to determine the Jacobian matrix given in Appendix A, and the derivatives

$$\frac{\partial \mathcal{C}_i\left(\widehat{f}_Q\right)}{\partial \widehat{Z}_j} = \frac{\zeta\,\Gamma_i(\widehat{f}_Q)}{\widehat{f}_Q}\,\frac{\partial\sqrt{h_i}}{\partial \widehat{Z}_j} \quad \text{for } i,j = 1\ldots n \tag{60}$$

$$\frac{\partial \mathcal{C}_i\left(\widehat{f}_Q\right)}{\partial \widehat{f}_Q} = -\frac{\zeta\,\Gamma_i(\widehat{f}_Q)}{\widehat{f}_Q^{\,2}}\,\sqrt{h_i} \quad \text{for } i = 0\ldots n+1 \tag{61}$$

required to determine the Jacobian matrix given in Appendix B. The functions $\Gamma_i$ in Eqs. (58) to (61) are given by

$$\Gamma_i(\widehat{f}_0) = \frac{1}{1 - 4\nu\,\mathcal{C}_i(\widehat{f}_0) + 3\nu^2\left[\mathcal{C}_i(\widehat{f}_0)\right]^2} \tag{62}$$

$$\Gamma_i(\widehat{f}_Q) = \frac{1}{1 - 4\nu\,\mathcal{C}_i(\widehat{f}_Q) + 3\nu^2\left[\mathcal{C}_i(\widehat{f}_Q)\right]^2} \tag{63}$$

For illustration purposes, we apply the proposed finite difference model to the example presented by Huddleston etal. (1994), consisting of a suspended cable spanning a horizontal distance $L = 100\,\text{m}$ and having an unstrained arc-length $\widetilde{S} = L$ as illustrated in Fig. 4 (a). The cable is subjected to its own weight $\widetilde{m}\text{g}$ per unit unstrained arc-length. The flowchart in Fig. 3 is applied using $P^{(k)} = 0$, $Q = 0$ and replacing $\widehat{f}_Q$ by $\widehat{f}_0$. The cable is then discretized into 100 finite difference elements and the NLS problem is solved for the vector $\boldsymbol{\chi}$ given by Eq. (36) as detailed in Section 2.1.2. Although a coarser discretization with fewer finite difference elements would yield satisfactory results at the nodes, a more refined mesh density corresponding to 1-m length finite difference cable elements is adopted to ensure an accurate static response along the whole cable arc-length. Since $\widetilde{S} = L$, we consider initial cable deflections $\widehat{z}_i^{(0)} = 0$, $i = 1\ldots n$, yielding the first $n$ elements of the starting vector $\boldsymbol{\chi}^{(0)}$. Taking account of the scaling discussed previously, the last element $\widehat{f}_0$ of vector $\boldsymbol{\chi}^{(0)}$ can be selected to have the same order of magnitude as the first $n$ elements of the same vector. For practical guidance, we recommend using the horizontal tension in a Hookean cable with rigid cross-section as a initial guess of horizontal tension and corresponding parameter $\widehat{f}_0$. This initial horizontal tension can be obtained either: (i) using available analytical expressions when only self-weight or simple loading cases are involved [3, 13], (ii) or by applying the flowchart in Fig. 3 with constitutive function $\mathcal{C}(\widehat{\tau}) = \widehat{\tau}$. In this case, the latter strategy is employed, and a horizontal tension $\widehat{H} = 1.82\,\text{kN}$ in a Hookean cable with rigid cross-section is first obtained using an initial horizontal tension $\widehat{H}^{(0)} = 10^{40}\,\text{kN}$ chosen intentionally high to illustrate the effectiveness of the finite difference scheme in converging to a much lower value of horizontal cable tension. The new initial horizontal tension $\widehat{H}^{(0)} = 1.82\,\text{kN}$ and corresponding parameter $\widehat{f}_0 = 0.342$ are then used as starting values for the analysis of the cable with deformable cross-section. The cable's static profiles obtained using the proposed method are presented in Fig. 5 for $\nu = 0.0$, $\nu = 0.2$ and $\nu = 0.4$. It can be seen that the obtained results are in excellent agreement with those reported by Huddleston etal. (1994). To characterize the maximum deflection of

the cable with respect to its chord, we define the nondimensional deflection indexes $\widehat{f}_{\text{max}}$

$$\widehat{f}_{\text{max}} = \frac{\max\left|\,\widehat{\mathbf{z}} - \widehat{\mathbf{z}}^{(\text{ch})}\right|}{L} \tag{64}$$

in which $\widehat{\mathbf{z}}$ denotes a vector containing the coordinates $\widehat{z}_i$, $i = 1 \ldots n$, of the interior finite difference nodes of the deflected cable, and $\widehat{\mathbf{z}}^{(\text{ch})}$ a vector containing the coordinates $\widehat{z}_i^{(\text{ch})}$, $i = 1 \ldots n$, of the vertical projections of the nodes on the chord of the cable as illustrated in Fig. 1 (b). The computed horizontal tensions $\widehat{H}$, strained arc-lengths $\widehat{S}$ and deflection indexes $\widehat{f}_{\text{max}}$ are presented in Table 1. To investigate the influence of chord inclination and additional loads, we apply the proposed method to determine the profiles of the previous cables along the inclined configuration shown in Fig. 4 (b). In this case, we assume that the unstrained arc-length is $\widetilde{S} = \sqrt{100^2 + 50^2} = 111.80\,\text{m}$. We also consider initial cable deflections $\widehat{z}_i^{(0)} = \widehat{z}_i^{(\text{ch})}$, $i = 1 \ldots n$, yielding the first $n$ elements of the starting vector $\boldsymbol{\chi}^{(0)}$. As previously, the initial horizontal tension $\widehat{H}^{(0)}$ and corresponding parameter $\widehat{f}_0$ are first estimated based on the response of a Hookean inclined suspended cable determined using the flowchart in Fig. 3 with constitutive function $\mathcal{C}(\widehat{\tau}) = \widehat{\tau}$, $z_{\text{B}} = 50\,\text{m}$, $P^{(1)} = 1\,\text{kN}$ and $Q^{(1)} = 0.1\,\text{kN/m}$. Fig. 6 illustrates the obtained results highlighting the effects of cross-sectional deformation on the static response of the cable hanging under self-weight only (Fig. 6 (a)) as well as under self-weight combined with concentrated and uniformly distributed loads (Fig. 6 (b)). The horizontal tensions $\widehat{H}$, strained arc-lengths $\widehat{S}$ and deflection indexes $\widehat{f}_{\text{max}}$ are also included in Table 1. Figs. 5-6 and Table 1 reveal that: (i) a higher Poisson's ration corresponds to decreasing horizontal tension and increasing arc-length as well as deflection index, and (ii) the effect of cross-section deformation is more important as the cable is inclined and then as vertical loads are applied.

### 3.3 Application to the analysis of cables made of neo-Hookean materials

As mentioned previously, most formulations in the literature focused on the behavior of cables made of Hookean materials, while cables made of nonlinear elastic materials such as rubber and rubber-like materials were rarely studied. To illustrate the versatility of the proposed method, we apply it next to study the response of suspended cables made of a neo-Hookean material, one of the most common constitutive models for rubber. In this case, we show that cable tension can be expressed as

$$\widehat{F} = GA\left\{1 + \mathcal{C}(\widehat{\tau}) - \frac{1}{\left[1 + \mathcal{C}(\widehat{\tau})\right]^2}\right\} \tag{65}$$

in which $G$ is the cable shear modulus which can be approximately related to the elastic modulus by $G = E/3$ [42, 43]. Then using Eq. (9), Eq. (65) becomes

$$\widehat{\tau} = \frac{1}{3}\left\{1 + \mathcal{C}(\widehat{\tau}) - \frac{1}{\left[1 + \mathcal{C}(\widehat{\tau})\right]^2}\right\} \tag{66}$$

which can be solved numerically or analytically using Cardano's formula. Following the same derivations as in the previous section, we show that Eqs. (54) to (56) and Eqs. (58) to (61) apply with the functions $\Gamma$ and $\Gamma_i$ now given by

$$\Gamma(\widehat{\tau}) = \frac{1 + \mathcal{C}(\widehat{\tau})}{1 - 2\,\widehat{\tau} + \mathcal{C}(\widehat{\tau})} \tag{67}$$

$$\Gamma_i(\widehat{f}_0) = \frac{\widehat{f}_0 \left[1 + \mathcal{C}_i(\widehat{f}_0)\right]}{\widehat{f}_0 - 2\,\zeta\sqrt{h_i} + \widehat{f}_0\,\mathcal{C}_i(\widehat{f}_0)} \tag{68}$$

$$\Gamma_i(\widehat{f}_Q) = \frac{\widehat{f}_Q \left[1 + \mathcal{C}_i(\widehat{f}_Q)\right]}{\widehat{f}_Q - 2\,\zeta\sqrt{h_i} + \widehat{f}_Q\,\mathcal{C}_i(\widehat{f}_Q)} \tag{69}$$

The proposed technique is applied to examples presented by Valiente (2006) who developed analytical expressions of the symmetric catenary of horizontal suspended cables made of neo-Hookean materials and hanging under self-weight as the one illustrated in Fig. 7 (a). The static profiles of horizontal suspended cables made of a neo-Hookean material and subjected to self-weight only are determined first using the proposed method and considering unstrained arc-length $\widetilde{S} = L$ and elastic moduli $E = \widetilde{m}\mathrm{g}L/(2A)$ and $E = \widetilde{m}\mathrm{g}L/(4A)$. For purpose of comparison, the static response of cables made of Hookean materials with the same elastic moduli are also illustrated. As previously, a mesh density corresponding to 1-m length finite difference cable elements is adopted to ensure an accurate static response along the whole cable arc-length. Therefore, the cables are discretized into 200 finite difference elements and the flowchart in Fig. 3 is applied using $P^{(k)} = 0$, $Q = 0$ and replacing $\widehat{f}_Q$ by $\widehat{f}_0$. The values of the starting vector $\boldsymbol{\chi}^{(0)}$ of the algorithm are selected using the same technique as described in the previous example. Fig. 7 reveals that the obtained static profiles are identical to those given by the analytical method developed by Valiente (2006). The effects of chord inclination and loading are illustrated next by applying the proposed technique to determine the static response of the inclined cable shown in Fig. 7 (b). In this case, we assume that the unstrained arc-length is $\widetilde{S} = \sqrt{200^2 + 50^2} = 206.15\,\mathrm{m}$ and that initial cable deflections are $\widehat{z}_i^{(0)} = \widehat{z}_i^{(\mathrm{ch})}$, $i = 1 \ldots n$. The flowchart in Fig. 3 is applied using $z_{\mathrm{B}} = 50\,\mathrm{m}$, $P^{(1)} = 500\,\mathrm{kN}$, $Q^{(1)} = 10\,\mathrm{kN/m}$ and an initial starting vector $\boldsymbol{\chi}^{(0)}$ estimated based on the response of a Hookean inclined suspended cable as described previously. The results obtained are presented in Fig. 9 (a) when the cable is subjected to self-weight only, and Fig. 9 (b) when the cable is subjected to concentrated and distributed loads in addition to self-weight. The horizontal tensions $\widehat{H}$, strained arc-lengths $\widehat{S}$ and deflection indexes $\widehat{f}_{\mathrm{max}}$ obtained for the Hookean and neo-Hookean cables studied are given in Table 2. It is clear from Figs. 8-9 and Table 2 that the differences between both types of cables are significant and become even more important as the cable is inclined and as vertical loads are applied. We note that these case studies are given here for illustration purposes assuming that the materials behave as Hookean or neo-Hookean up to maximum deflection. For each particular case, the analyst has to verify that the computed strains are within the limits of applicability of Hookean, neo-Hookean or other nonlinear elastic behavior.

## 4 Conclusions

An original and practical formulation and finite difference scheme were developed to investigate the static response of horizontal and inclined cables with deformable cross-section, made of general linear or nonlinear elastic materials, and subjected to vertical concentrated and distributed loads. The proposed formulation also includes large sag and extensibility effects. Considering various loading cases, we showed that the resulting nonlinear system of equations can be transformed into a nonlinear least squares problem that can be solved efficiently to determine the nonlinear static response of suspended cables made of nonlinear elastic materials. The proposed technique was programmed and its application was illustrated through examples highlighting the effects of coupling between the tension in a cable and the deformation of its cross-section as well as the use of a neo-Hookean material. The obtained results were successfully validated against analytical solutions when available. The proposed technique can be easily programmed and presents a valuable and effective alternative to finite element analysis when implementation of general constitutive nonlinear elastic material models is not straightforward and recourse to cumbersome 3D cable modeling using solid finite elements is to be avoided.

## Acknowledgements

The authors would like to acknowledge the financial support of the Natural Sciences and Engineering Research Council of Canada (NSERC).

## Appendix A

In this Appendix, we propose analytical expressions to determine the the non-zero elements of the Jacobian matrice $\mathbf{J}_{\boldsymbol{\eta}^{(\ell)}}$ given by Eq. (40). The superscript $^{(\ell)}$ is omitted herein to alleviate the text.

$$\frac{\partial \eta_i}{\partial \widehat{Z}_{i-1}} = \left(n+1\right)^2 - \frac{4\left(n+1\right)\widehat{f}_0\, a_i}{\left[1+\mathcal{C}_i\left(\widehat{f}_0\right)\right]\sqrt{h_i}} - \frac{8\,\widehat{f}_0\sqrt{h_i}}{\left[1+\mathcal{C}_i\left(\widehat{f}_0\right)\right]^2}\,\frac{\partial \mathcal{C}_i\left(\widehat{f}_0\right)}{\partial \widehat{Z}_{i-1}} \qquad \text{for } i = 2\ldots n \qquad \text{(A1)}$$

$$\frac{\partial \eta_i}{\partial \widehat{Z}_i} = -2\left(n+1\right)^2 - \frac{8\,\widehat{f}_0\sqrt{h_i}}{\left[1+\mathcal{C}_i\left(\widehat{f}_0\right)\right]^2}\,\frac{\partial \mathcal{C}_i\left(\widehat{f}_0\right)}{\partial \widehat{Z}_i} \qquad \text{for } i = 1\ldots n \qquad \text{(A2)}$$

$$\frac{\partial \eta_i}{\partial \widehat{Z}_{i+1}} = \left(n+1\right)^2 + \frac{4\left(n+1\right)\widehat{f}_0\, a_i}{\left[1+\mathcal{C}_i\left(\widehat{f}_0\right)\right]\sqrt{h_i}} - \frac{8\,\widehat{f}_0\sqrt{h_i}}{\left[1+\mathcal{C}_i\left(\widehat{f}_0\right)\right]^2}\,\frac{\partial \mathcal{C}_i\left(\widehat{f}_0\right)}{\partial \widehat{Z}_{i+1}} \qquad \text{for } i = 1\ldots n-1 \qquad \text{(A3)}$$

$$\frac{\partial \eta_i}{\partial \widehat{f}_0} = \frac{8\sqrt{h_i}}{\left[1+\mathcal{C}_i\left(\widehat{f}_0\right)\right]}\left\{1 - \frac{\widehat{f}_0}{\left[1+\mathcal{C}_i\left(\widehat{f}_0\right)\right]}\,\frac{\partial \mathcal{C}_i\left(\widehat{f}_0\right)}{\partial \widehat{f}_0}\right\} \qquad \text{for } i = 1\ldots n \qquad \text{(A4)}$$

$$\frac{\partial \eta_{n+1}}{\partial \widehat{Z}_i} = \frac{1}{\left(n+1\right)}\sum_{j=i-2}^{i+3}\frac{1}{\left(1+\varepsilon_j\right)}\left[\frac{\kappa_j}{\sqrt{1+\kappa_j^2}}\,\frac{\partial \kappa_j}{\partial \widehat{Z}_i} - \frac{\sqrt{1+\kappa_j^2}}{\left(1+\varepsilon_j\right)}\,\frac{\partial \varepsilon_j}{\partial \widehat{Z}_i}\right] \qquad \text{for } i = 3\ldots n-2 \qquad \text{(A5)}$$

$$\frac{\partial \eta_{n+1}}{\partial \widehat{Z}_1} = \frac{1}{\left(n+1\right)}\sum_{j=1}^{3}\frac{1}{\left(1+\varepsilon_j\right)}\left[\frac{\kappa_j}{\sqrt{1+\kappa_j^2}}\,\frac{\partial \kappa_j}{\partial \widehat{Z}_1} - \frac{\sqrt{1+\kappa_j^2}}{\left(1+\varepsilon_j\right)}\,\frac{\partial \varepsilon_j}{\partial \widehat{Z}_1}\right] \qquad \text{(A6)}$$

$$\frac{\partial \eta_{n+1}}{\partial \widehat{Z}_2} = \frac{1}{\left(n+1\right)}\sum_{j=1}^{4}\frac{1}{\left(1+\varepsilon_j\right)}\left[\frac{\kappa_j}{\sqrt{1+\kappa_j^2}}\,\frac{\partial \kappa_j}{\partial \widehat{Z}_2} - \frac{\sqrt{1+\kappa_j^2}}{\left(1+\varepsilon_j\right)}\,\frac{\partial \varepsilon_j}{\partial \widehat{Z}_2}\right] \qquad \text{(A7)}$$

$$\frac{\partial \eta_{n+1}}{\partial \widehat{Z}_{n-1}} = \frac{1}{\left(n+1\right)}\sum_{j=n-3}^{n+1}\frac{1}{\left(1+\varepsilon_j\right)}\left[\frac{\kappa_j}{\sqrt{1+\kappa_j^2}}\,\frac{\partial \kappa_j}{\partial \widehat{Z}_{n-1}} - \frac{\sqrt{1+\kappa_j^2}}{\left(1+\varepsilon_j\right)}\,\frac{\partial \varepsilon_j}{\partial \widehat{Z}_{n-1}}\right] \qquad \text{(A8)}$$

$$\frac{\partial \eta_{n+1}}{\partial \widehat{Z}_n} = \frac{1}{\left(n+1\right)}\sum_{j=n-2}^{n+1}\frac{1}{\left(1+\varepsilon_j\right)}\left[\frac{\kappa_j}{\sqrt{1+\kappa_j^2}}\,\frac{\partial \kappa_j}{\partial \widehat{Z}_n} - \frac{\sqrt{1+\kappa_j^2}}{\left(1+\varepsilon_j\right)}\,\frac{\partial \varepsilon_j}{\partial \widehat{Z}_n}\right] \qquad \text{(A9)}$$

$$\frac{\partial \eta_{n+1}}{\partial \widehat{f}_0} = -\frac{1}{2\left(n+1\right)}\sum_{j=1}^{n+1}\frac{\sqrt{1+\kappa_j^2}}{\left(1+\varepsilon_j\right)^2}\left[\frac{\partial \mathcal{C}_{j-1}\left(\widehat{f}_0\right)}{\partial \widehat{f}_0} + \frac{\partial \mathcal{C}_j\left(\widehat{f}_0\right)}{\partial \widehat{f}_0}\right] \qquad \text{(A10)}$$

## Appendix B

In this Appendix, we propose analytical expressions to determine the non-zero elements of the Jacobian matrice $\mathbf{J}_{\boldsymbol{\eta}^{(\ell)}}$ when the effects cable self-weight are combined with concentrated and distributed loads as discussed in Section 2.2. The superscript $^{(\ell)}$ is omitted herein to alleviate the text.

$$\frac{\partial \eta_i}{\partial \widehat{Z}_{i-1}} = \left(n+1\right)^2 - \frac{4\left(n+1\right)\widehat{f}_i\, a_i}{\left[1+\mathcal{C}_i(\widehat{f}_Q)\right]\sqrt{h_i}} - \frac{8\,\widehat{f}_i\sqrt{h_i}}{\left[1+\mathcal{C}_i(\widehat{f}_Q)\right]^2}\frac{\partial \mathcal{C}_i(\widehat{f}_Q)}{\partial \widehat{Z}_{i-1}} \qquad \text{for } i=2\ldots n \tag{B1}$$

$$\frac{\partial \eta_i}{\partial \widehat{Z}_i} = -2\left(n+1\right)^2 - \frac{8\,\widehat{f}_i\sqrt{h_i}}{\left[1+\mathcal{C}_i(\widehat{f}_Q)\right]^2}\frac{\partial \mathcal{C}_i(\widehat{f}_Q)}{\partial \widehat{Z}_i} \qquad \text{for } i=1\ldots n \tag{B2}$$

$$\frac{\partial \eta_i}{\partial \widehat{Z}_{i+1}} = \left(n+1\right)^2 + \frac{4\left(n+1\right)\widehat{f}_i\, a_i}{\left[1+\mathcal{C}_i(\widehat{f}_Q)\right]\sqrt{h_i}} - \frac{8\,\widehat{f}_i\sqrt{h_i}}{\left[1+\mathcal{C}_i(\widehat{f}_Q)\right]^2}\frac{\partial \mathcal{C}_i(\widehat{f}_Q)}{\partial \widehat{Z}_{i+1}} \qquad \text{for } i=1\ldots n-1 \tag{B3}$$

$$\begin{aligned}\frac{\partial \eta_i}{\partial \widehat{f}_Q} &= \frac{8\sqrt{h_i}}{\left[1+\mathcal{C}_i(\widehat{f}_Q)\right]}\left\{1 - \frac{\widehat{f}_i}{\left[1+\mathcal{C}_i(\widehat{f}_Q)\right]}\frac{\partial \mathcal{C}_i(\widehat{f}_Q)}{\partial \widehat{f}_Q}\right\} && \text{for } i=1\ldots n \\ &+ \frac{8\left(n+1\right)P^{(k)}}{L\left(\widetilde{m}\mathrm{g}+Q\right)} && \text{if } i=p^{(k)}\end{aligned} \tag{B4}$$

$$\frac{\partial \eta_{n+1}}{\partial \widehat{Z}_i} = \frac{1}{\left(n+1\right)}\sum_{j=i-2}^{i+3}\frac{1}{\left(1+\varepsilon_j\right)}\left[\frac{\kappa_j}{\sqrt{1+\kappa_j^2}}\frac{\partial \kappa_j}{\partial \widehat{Z}_i} - \frac{\sqrt{1+\kappa_j^2}}{\left(1+\varepsilon_j\right)}\frac{\partial \varepsilon_j}{\partial \widehat{Z}_i}\right] \qquad \text{for } i=3\ldots n-2 \tag{B5}$$

$$\frac{\partial \eta_{n+1}}{\partial \widehat{Z}_1} = \frac{1}{\left(n+1\right)}\sum_{j=1}^{3}\frac{1}{\left(1+\varepsilon_j\right)}\left[\frac{\kappa_j}{\sqrt{1+\kappa_j^2}}\frac{\partial \kappa_j}{\partial \widehat{Z}_1} - \frac{\sqrt{1+\kappa_j^2}}{\left(1+\varepsilon_j\right)}\frac{\partial \varepsilon_j}{\partial \widehat{Z}_1}\right] \tag{B6}$$

$$\frac{\partial \eta_{n+1}}{\partial \widehat{Z}_2} = \frac{1}{\left(n+1\right)}\sum_{j=1}^{4}\frac{1}{\left(1+\varepsilon_j\right)}\left[\frac{\kappa_j}{\sqrt{1+\kappa_j^2}}\frac{\partial \kappa_j}{\partial \widehat{Z}_2} - \frac{\sqrt{1+\kappa_j^2}}{\left(1+\varepsilon_j\right)}\frac{\partial \varepsilon_j}{\partial \widehat{Z}_2}\right] \tag{B7}$$

$$\frac{\partial \eta_{n+1}}{\partial \widehat{Z}_{n-1}} = \frac{1}{\left(n+1\right)}\sum_{j=n-3}^{n+1}\frac{1}{\left(1+\varepsilon_j\right)}\left[\frac{\kappa_j}{\sqrt{1+\kappa_j^2}}\frac{\partial \kappa_j}{\partial \widehat{Z}_{n-1}} - \frac{\sqrt{1+\kappa_j^2}}{\left(1+\varepsilon_j\right)}\frac{\partial \varepsilon_j}{\partial \widehat{Z}_{n-1}}\right] \tag{B8}$$

$$\frac{\partial \eta_{n+1}}{\partial \widehat{Z}_n} = \frac{1}{\left(n+1\right)}\sum_{j=n-2}^{n+1}\frac{1}{\left(1+\varepsilon_j\right)}\left[\frac{\kappa_j}{\sqrt{1+\kappa_j^2}}\frac{\partial \kappa_j}{\partial \widehat{Z}_n} - \frac{\sqrt{1+\kappa_j^2}}{\left(1+\varepsilon_j\right)}\frac{\partial \varepsilon_j}{\partial \widehat{Z}_n}\right] \tag{B9}$$

$$\frac{\partial \eta_{n+1}}{\partial \widehat{f}_Q} = -\frac{1}{2\left(n+1\right)}\sum_{j=1}^{n+1}\frac{\sqrt{1+\kappa_j^2}}{\left(1+\varepsilon_j\right)^2}\left[\frac{\partial \mathcal{C}_{j-1}(\widehat{f}_Q)}{\partial \widehat{f}_Q} + \frac{\partial \mathcal{C}_j(\widehat{f}_Q)}{\partial \widehat{f}_Q}\right] \tag{B10}$$

## References


Truesdell CA. The rational mechanics of flexible or elastic bodies, 1638-1788, Leonardo Euleri Opera Omnia, series II, vol. II, part 2. Zurich, Orell Füssli; 1960.

Truesdell CA. Essays in the history of mechanics. New York, Springer; 1968.

Irvine HM. Cable structures. Cambridge, The MIT Press; 1981.

O'Brien T, Francis AJ. Cable movements under two-dimensional loads. Journal of the Structural Division, ASCE 1964; ST3:89-123.

O'Brien T. General solution of suspended cable problems. Journal of the Structural Division, ASCE 1967; ST1:1-26.

Ernst JH. Der E-modul von seilen unter Berucksichtigung des durchhanges. Bauingenieur 1965; 40:52–55.

Irvine HM, Sinclair GB. The suspended elastic cable under the action of concentrated vertical loads. International Journal of Solids and Structures 1972; 12:309-317.

Irvine HM. Statics of suspended cables. Journal of the Engineering Mechanics Division, ASCE 1975; 101:187-205.

Gambhir ML, Batchelor BA. A finite element for 3-D prestressed cablenets. International Journal for Numerical Methods in Engineering 1977; 11:1699-1718.

Peyrot AH, Goulois AM. Analysis of cable structures. Journal of Computers and Structures 1979; 10:805-813.

Huddleston JV. Computer analysis of extensible cables. Journal of the Engineering Mechanics Division, ASCE 1981; 107:27-37.

Jayaraman HB, Knudson WC. A curve element for the analysis of cable structures. Journal of Computers and Structures 1981; 14:325-333.

Leonard JW. Tension structures. New York, McGraw-Hill; 1988.

Huddleston JV, Ham HJ. Poisson effect in flexible cables with both ends fixed. Journal of Engineering Mechanics, ASCE 1994; 120:1590-1595.

Karoumi R. Some modeling aspects in the nonlinear finite element analysis of cable supported bridges. Journal of Computers and Structures 1999; 71:397-412.

Sagatun SI. The elastic cable under the action of concentrated and distributed forces. Journal of Offshore Mechanics and Arctic Engineering 2001; 123:43-45.

Chucheepsakul S, Srinil N, Petchpeart P. A variational approach for three-dimensional model of extensible marine cables with specified top tension. Journal of Applied Mathematical Modelling 2003; 27:781–803.

Andreu A, Gil L, Roca P. A new deformable catenary element for the analysis of cable net structures. Journal of Computers and Structures 2006; 84:1882–1890.

Freire AMS, Negra JHO, Lopes AV. Geometrical nonlinearities on the static analysis of highly flexible steel cable-stayed bridges. Journal of Computers and Structures 2006; 84:2128–2140.

Huang Y, Lan WR. Static analysis of cable structures. Applied Mathematics and Mechanics 2006; 27:1425–1430.

Ren WX, Huang MG, Hu WH. A parabolic cable element for static analysis of cable structures. Journal of Engineering Computations 2008; 25:366-384.

Vallabhan CVG. Two-dimensional nonlinear analysis of long cables. Journal of Engineering Mechanics, ASCE 2008; 134:694–697.

Matheson MJ, Holmes JD. Simulation of the dynamic response of transmission lines in strong winds. Journal of Engineering Structures 1981; 3:105–110.

Palucha MJ, Cappellarib TTO, Rierac JD. Experimental and numerical assessment of EPS wind action on long span transmission line conductors. Journal of Wind Engineering and Industrial Aerodynamics 2007; 95:473–492.

Luongo A, Zulli D, Piccardo G. Analytical and numerical approaches to nonlinear galloping of internally resonant suspended cables. Journal of Sound and Vibration 2008; 315:375-93.

Ablow CM, Schechter S. Numerical simulation of undersea cable dynamics. Journal of Ocean Engineering 1983; 10:443–457.

Tjavaras AA, Zhu Q, Liu Y, Triantafyllou MS, and Yue DKP. The mechanics of highly-extensible cables. Journal of Sound and Vibration 1998; 213:709–737.

Feng Z, Allen R. Evaluation of the effects of the communication cable on the dynamics of an underwater flight vehicle. Journal of Ocean Engineering 2004; 31:1019–1035.

Bouaanani N. Numerical investigation of the modal sensitivity of suspended cables with localized damage. Journal of Sound and Vibration 2006; 292:1015–1030.

Mehrabi AB, Tabatabai H. Unified finite difference formulation for free vibration of cables. Journal of Structural Engineering 1998; 124:1313-1322.

Hua XG, Ni YQ, Chen ZQ, Ko JM. Structural damage detection of cable-stayed bridges using changes in cable forces and model updating. Journal of Structural Engineering 2009; 135:1093-1106.

Bruno D, Greco F, Lonetti P. A parametric study on the dynamic behavior of combined cable-stayed and suspension bridges under moving loads. International Journal for Computational Methods in Engineering Science and Mechanics 2009; 10:243–258.

Bruno D, Leonardi A. Nonlinear structural models in cableway transport systems. Simulation Practice and Theory 1999; 7:207-218.

Ni YQ, Ko JM, Zheng G. Dynamic analysis of large-diameter sagged cables taking into account flexural rigidity. Journal of Sound and Vibration 2002; 257:301-319.

Srinil N, Rega G, Chucheepsakul S. Large amplitude three-dimensional free vibrations of inclined sagged elastic cables. Nonlinear Dynamics 2003; 33:129-154.

Kozak K, Zhou Q, Wang J. Static analysis of cable-driven manipulators with non-negligible cable mass. IEEE Transactions on Robotics 2006; 22:425-433.

Lopez-Garcia O, Carnicero A, Torres V, Jimenez-Octavio JR. The influence of cable slackening on the stiffness computation of railway overheads. International Journal of Mechanical Sciences 2008; 50:1213-1223.

Fan F., Jin XF, Shen SZ. Effect of non-uniform solar temperature field on cable-net structure of reflector of large radio telescope-FAST. Advances in Structural Engineering 2009; 12:503-512.

MATLAB ® The Mathworks, Inc., Natick, MA; 2009.

Dennis Jr JE, Schnabel RB. Numerical Methods for Unconstrained Optimization and Nonlinear Equations. Prentice-Hall, Englewood Cliffs, NJ; 1983.

Nayfeh AH, Pai PF. Linear and Nonlinear Structural Mechanics. Wiley-Interscience, Hoboken, NJ; 2004.

Ogden RW. Non-linear elastic deformations. Dover, New York; 1997.

Gent AN (Ed.). Engineering with Rubber, How to Design Rubber Component, Second edition. Hanser Gardner Publishers; 2001.

Valiente A. Symmetric Catenary of a Uniform Elastic Cable of Neo-Hookean Material. ASCE Journal of Engineering Mechanics 2006; 132:747-753.

## List of tables

Table 1
Effect of cross-sectional deformability on the static response of horizontal and inclined suspended cables subjected to vertical loads.

| Poisson's ratio | Self-weight only | | | | | | Self-weight and vertical loads | | |
|---|---|---|---|---|---|---|---|---|---|
| | Horizontal cable | | | Inclined cable | | | Inclined cable | | |
| | $\widehat{H}$ (kN) | $\widehat{S}$ (m) | $\widehat{f}_{\max}$ | $\widehat{H}$ (kN) | $\widehat{S}$ (m) | $\widehat{f}_{\max}$ | $\widehat{H}$ (kN) | $\widehat{S}$ (m) | $\widehat{f}_{\max}$ |
| $\nu=0.0$ | 1.82 | 122.92 | 0.317 | 1.62 | 138.89 | 0.394 | 2.41 | 156.57 | 0.518 |
| $\nu=0.2$ | 1.74 | 124.75 | 0.331 | 1.55 | 141.34 | 0.413 | 2.18 | 165.38 | 0.576 |
| $\nu=0.4$ | 1.64 | 127.51 | 0.352 | 1.42 | 146.71 | 0.453 | 1.94 | 176.61 | 0.647 |

Table 2
Static response of horizontal and inclined suspended cables made of a neo-Hookean material and subjected to vertical loads.

| Modulus of elasticity | Self-weight only | | | | | | Self-weight and vertical loads | | |
|---|---|---|---|---|---|---|---|---|---|
| | Horizontal cable | | | Inclined cable | | | Inclined cable | | |
| | $\widehat{H}$ (kN) | $\widehat{S}$ (m) | $\widehat{f}_{\max}$ | $\widehat{H}$ (kN) | $\widehat{S}$ (m) | $\widehat{f}_{\max}$ | $\widehat{H}$ (kN) | $\widehat{S}$ (m) | $\widehat{f}_{\max}$ |
| Hookean cable | | | | | | | | | |
| $E=\widetilde{m}\mathrm{g}L/(2A)$ | 366.42 | 329.71 | 0.599 | 355.96 | 342.69 | 0.634 | 448.01 | 419.30 | 0.855 |
| $E=\widetilde{m}\mathrm{g}L/(4A)$ | 242.46 | 430.76 | 0.893 | 235.89 | 449.73 | 0.944 | 283.55 | 600.88 | 1.350 |
| Neo-Hookean cable | | | | | | | | | |
| $E=\widetilde{m}\mathrm{g}L/(2A)$ | 268.81 | 412.88 | 0.845 | 260.43 | 432.60 | 0.898 | 284.17 | 630.59 | 1.432 |
| $E=\widetilde{m}\mathrm{g}L/(4A)$ | 149.85 | 674.56 | 1.556 | 145.30 | 711.89 | 1.653 | 151.30 | 1146.55 | 2.771 |

## List of figures

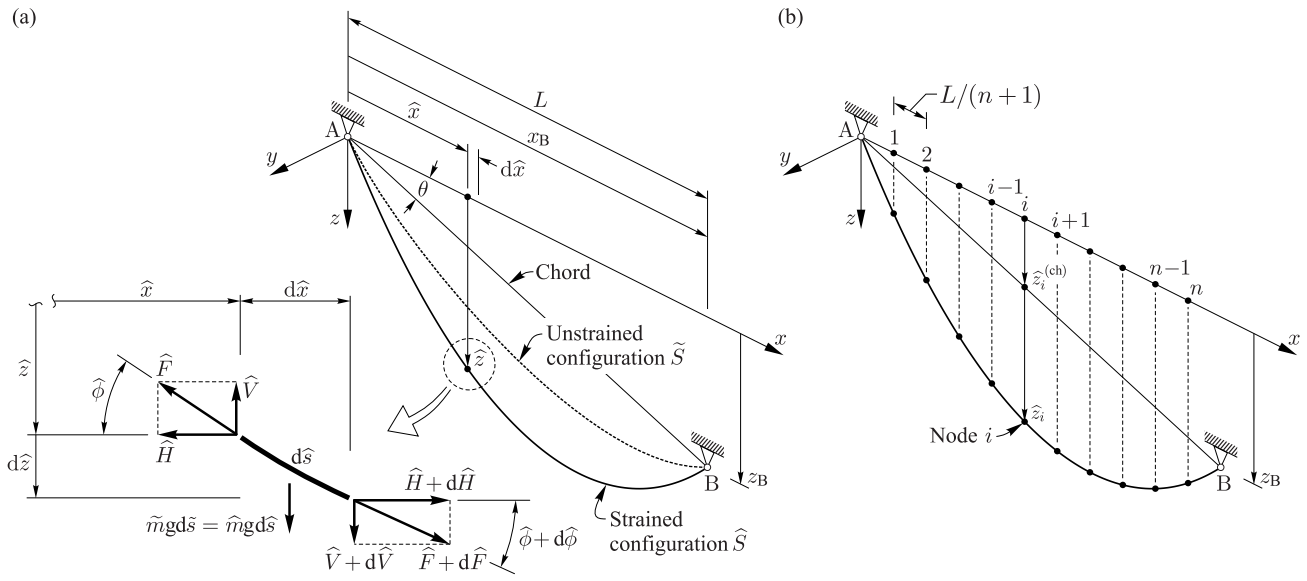


Figure 1. Static response of a suspended cable: (a) Unstrained and strained geometrical configurations and equilibrium of an elementary segment of the cable; (b) Finite difference mesh.

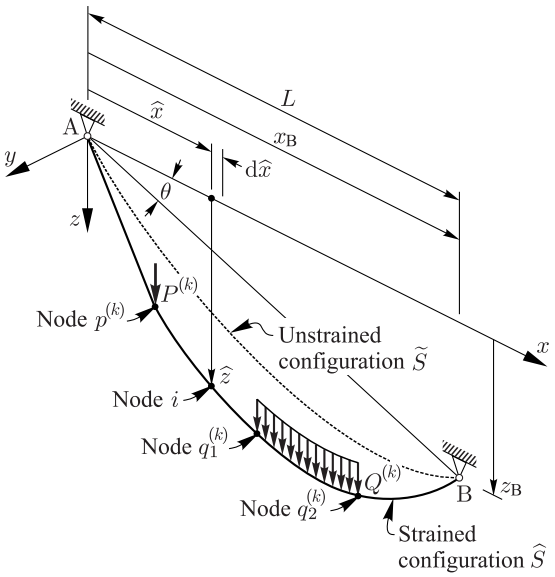


Figure 2. Suspended cable subjected to self-weight and to vertical concentrated and uniformly distributed loads.

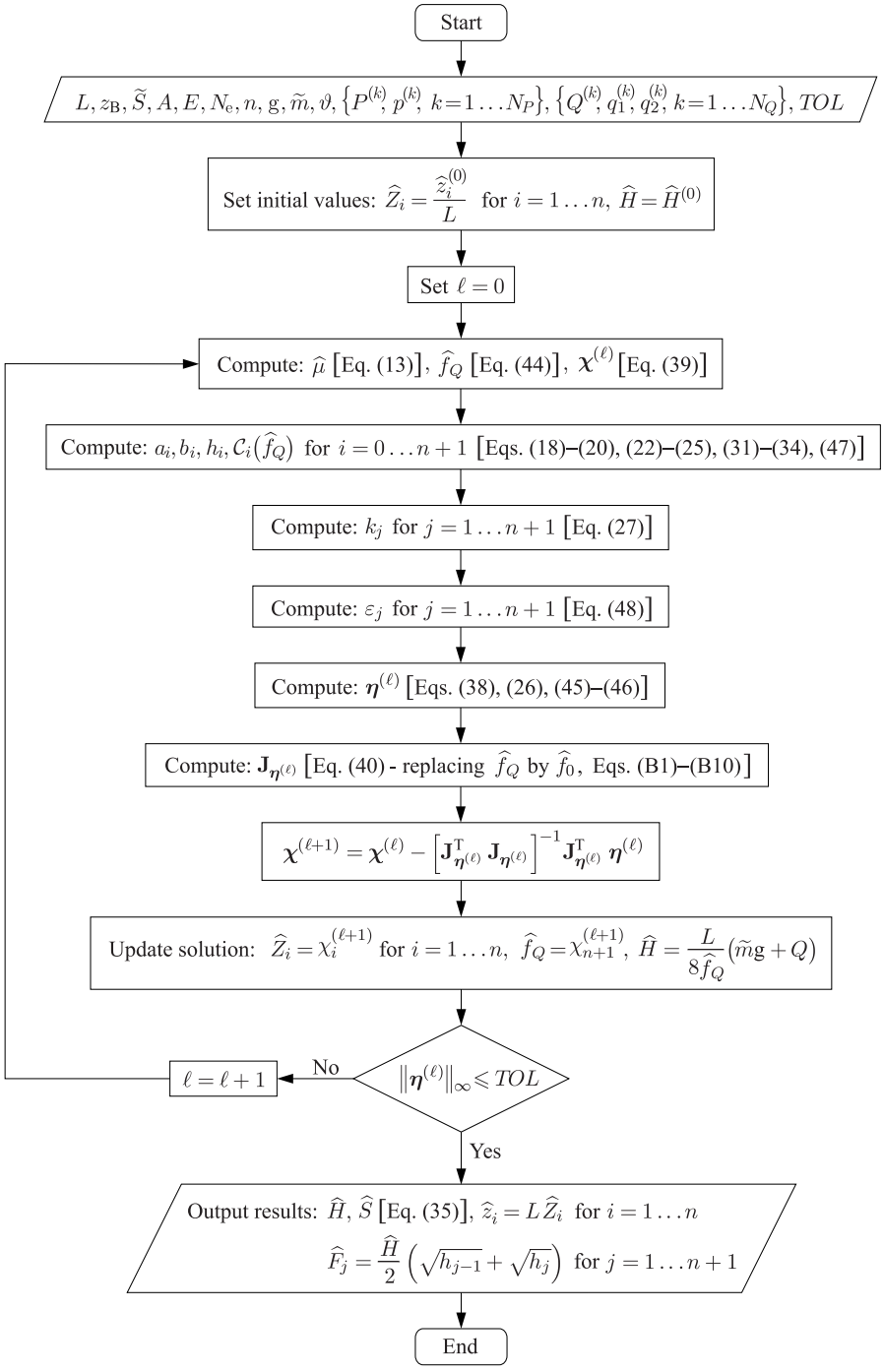


Figure 3. Flowchart illustrating the application of the finite difference scheme to suspended cables subjected to self-weight, and vertical concentrated and uniformly distributed loads.

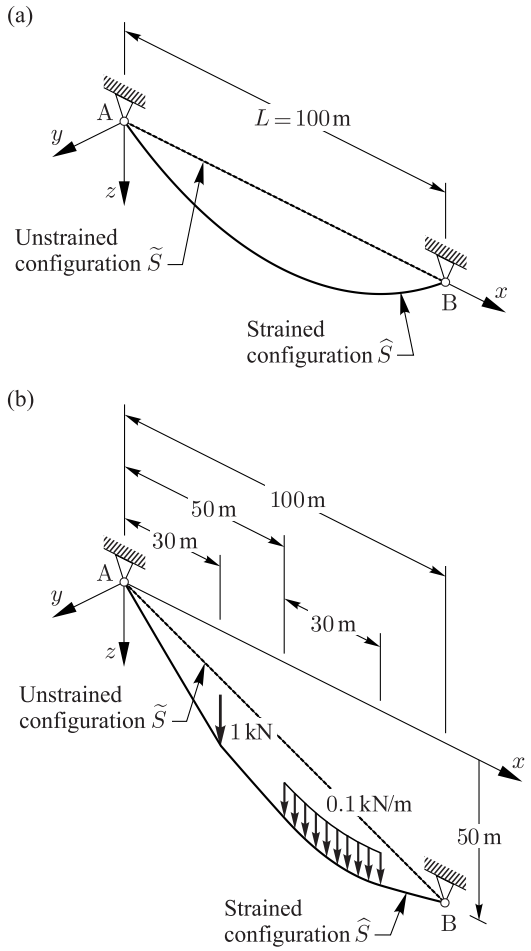


Figure 4. Suspended cables with deformable cross-section: (a) Horizontal cable hanging under self-weight only; (b) Inclined cable hanging under self-weight, concentrated and distributed loads.

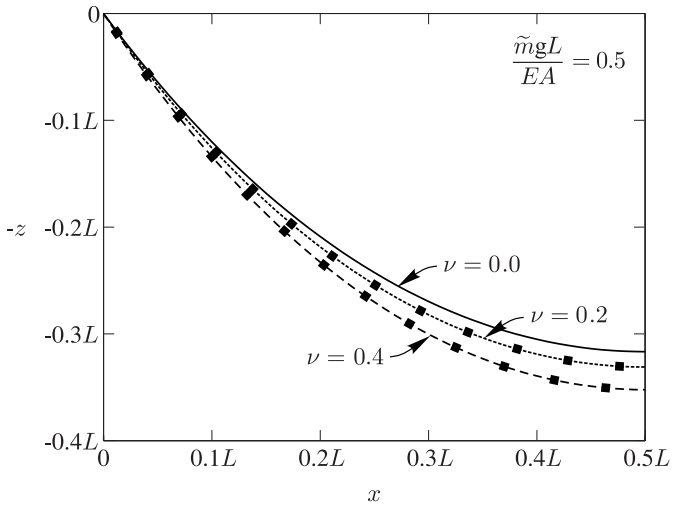


Figure 5. Effect of cross-sectional deformability on the static response of a horizontal suspended cable hanging under self-weight only. ——, – – –, ------ : Proposed method; -■-, – ■ – : Results from Huddleston etal. (1994).

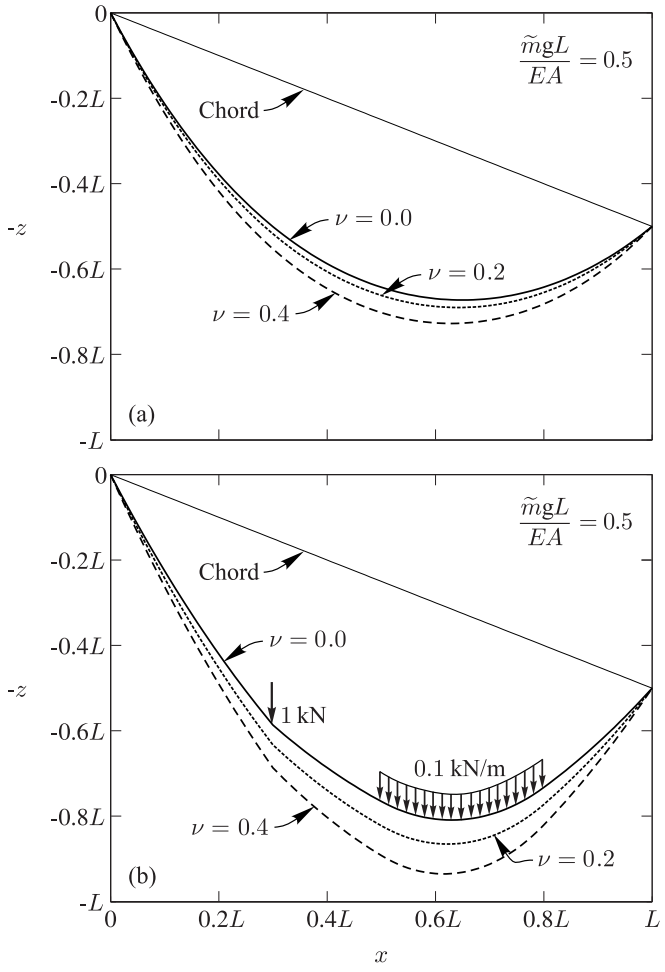


Figure 6. Effect of cross-sectional deformability on the static response of inclined suspended cables: (a) hanging under self-weight only; (b) hanging under self-weight, concentrated and distributed loads.

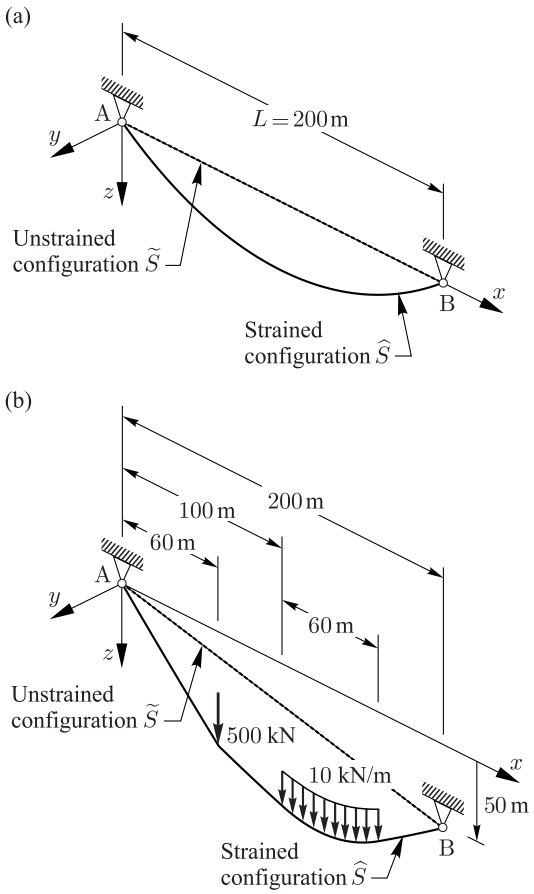


Figure 7. Suspended cables made of a Neo-Hookean material: (a) Horizontal cable hanging under self-weight only; (b) Inclined cable hanging under self-weight, concentrated and distributed loads.

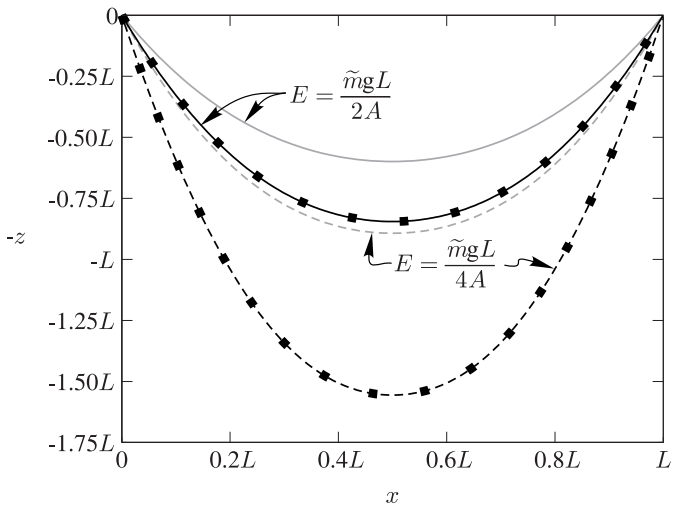


Figure 8. Static response of horizontal suspended cables made of Hookean and Neo-Hookean materials and hanging under self-weight only. ——, - - - : Proposed method (Hookean material); ——, - - - : Proposed method (Neo-Hookean material); —■—, - -■- - : Results from Valiente (2006) (Neo-Hookean material).

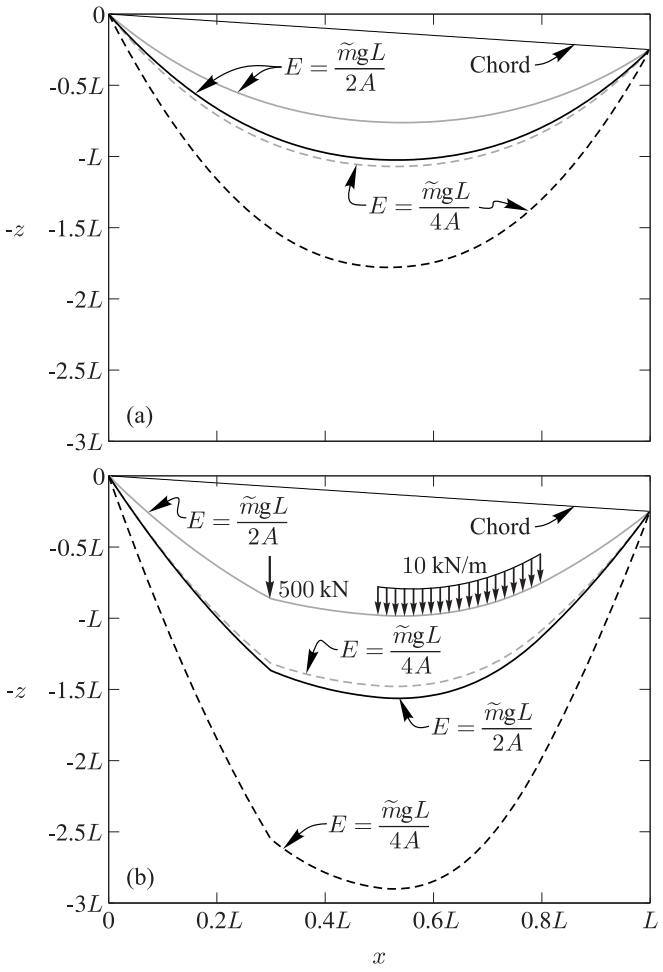


Figure 9. Static response of inclined suspended cables made of Hookean and Neo-Hookean materials: (a) hanging under self-weight only; (b) hanging under self-weight, concentrated and distributed loads. ——, – – – : Proposed method (Hookean material); ——, – – – : Proposed method (Neo-Hookean material).